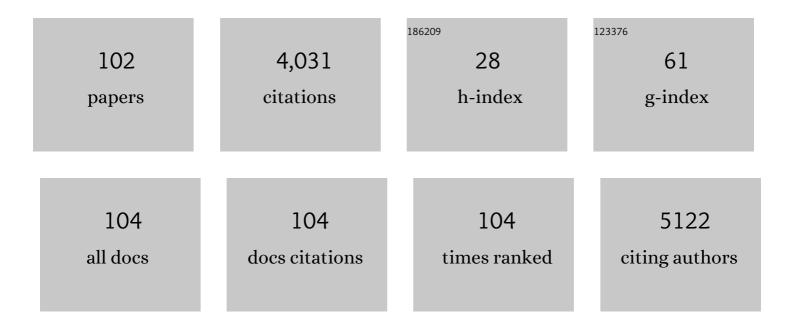
List of Publications by Year in descending order

Source: https://exaly.com/author-pdf/7170777/publications.pdf Version: 2024-02-01



LININA KIM

#	Article	IF	CITATIONS
1	Benign and Malignant Thyroid Nodules: US Differentiation—Multicenter Retrospective Study. Radiology, 2008, 247, 762-770.	3.6	935
2	Pediatric diffusion tensor imaging: Normal database and observation of the white matter maturation in early childhood. NeuroImage, 2006, 29, 493-504.	2.1	383
3	Preoperative Staging of Papillary Thyroid Carcinoma: Comparison of Ultrasound Imaging and CT. American Journal of Roentgenology, 2009, 193, 871-878.	1.0	279
4	Diffusion-Tensor MR Imaging and Fiber Tractography: A New Method of Describing Aberrant Fiber Connections in Developmental CNS Anomalies. Radiographics, 2005, 25, 53-65.	1.4	265
5	Stent-assisted coil embolization of intracranial wide-necked aneurysms. Neuroradiology, 2005, 47, 680-689.	1.1	140
6	Fully automated hybrid approach to predict the <i>IDH</i> mutation status of gliomas via deep learning and radiomics. Neuro-Oncology, 2021, 23, 304-313.	0.6	114
7	Pitfalls, Artifacts, and Remedies in Multi– Detector Row CT Coronary Angiography. Radiographics, 2004, 24, 787-800.	1.4	95
8	Surgical Treatment of Carotid Body Paragangliomas: Outcomes and Complications According to the Shamblin Classification. Clinical and Experimental Otorhinolaryngology, 2010, 3, 91.	1.1	93
9	Diffusion tensor MRI visualizes decreased subcortical fiber connectivity in focal cortical dysplasia. NeuroImage, 2004, 22, 1826-1829.	2.1	78
10	Visualization of endolymphatic hydrops and correlation with audio-vestibular functional testing in patients with definite Meniere's disease. Auris Nasus Larynx, 2013, 40, 167-172.	0.5	73
11	Glioma Grading Capability: Comparisons among Parameters from Dynamic Contrast-Enhanced MRI and ADC Value on DWI. Korean Journal of Radiology, 2013, 14, 487.	1.5	67
12	Characteristic sonographic findings of Warthin's tumor in the parotid gland. Journal of Clinical Ultrasound, 2004, 32, 78-81.	0.4	61
13	Alterations of white matter diffusion anisotropy in early deafness. NeuroReport, 2009, 20, 1032-1036.	0.6	57
14	Radiologic characteristics of sinonasal fungus ball: an analysis of 119 cases. Acta Radiologica, 2011, 52, 790-795.	0.5	57
15	Decreased fractional anisotropy of middle cerebellar peduncle in crossed cerebellar diaschisis: diffusion-tensor imaging-positron-emission tomography correlation study. American Journal of Neuroradiology, 2005, 26, 2224-8.	1.2	51
16	Value of CT added to ultrasonography for the diagnosis of lymph node metastasis in patients with thyroid cancer. Head and Neck, 2018, 40, 2137-2148.	0.9	48
17	Sonographically Guided Fine-Needle Aspiration Biopsy of Major Salivary Gland Masses: A Review of 245 Cases. American Journal of Roentgenology, 2011, 196, 1160-1163.	1.0	46
18	Clinical significance of quantitative analysis of facial nerve enhancement on MRI in Bell's palsy. Acta Oto-Laryngologica, 2008, 128, 1259-1265.	0.3	44

#	Article	IF	CITATIONS
19	Detection of Small Metastatic Brain Tumors. Investigative Radiology, 2012, 47, 136-141.	3.5	41
20	The cochleovestibular nerve identified during auditory brainstem implantation in patients with narrow internal auditory canals: Can preoperative evaluation predict cochleovestibular nerve deficiency?. Laryngoscope, 2011, 121, 1773-1779.	1.1	38
21	Correlation between MRI and Operative Findings in Bell's Palsy and Ramsay Hunt Syndrome. Yonsei Medical Journal, 2007, 48, 963.	0.9	37
22	The Prevalence and Features of Thyroid Pyramidal Lobe, Accessory Thyroid, and Ectopic Thyroid as Assessed by Computed Tomography: A Multicenter Study. Thyroid, 2013, 23, 84-91.	2.4	36
23	Application of Dynamic Contrast-Enhanced MRI Parameters for Differentiating Squamous Cell Carcinoma and Malignant Lymphoma of the Oropharynx. American Journal of Roentgenology, 2016, 206, 401-407.	1.0	34
24	Comparing quantitative tractography metrics of motor and sensory pathways in children with periventricular leukomalacia and different levels of gross motor function. Neuroradiology, 2012, 54, 615-621.	1.1	33
25	The change of hippocampal volume and its relevance with inner ear function in Meniere's disease patients. Auris Nasus Larynx, 2016, 43, 620-625.	0.5	32
26	Transoral robotic surgery for neurogenic tumors of the prestyloid parapharyngeal space. Auris Nasus Larynx, 2012, 39, 434-437.	0.5	31
27	Gadolinium deposition in the brain: association with various GBCAs using a generalized additive model. European Radiology, 2017, 27, 3353-3361.	2.3	29
28	Quality Reporting of Radiomics Analysis in Mild Cognitive Impairment and Alzheimer's Disease: A Roadmap for Moving Forward. Korean Journal of Radiology, 2020, 21, 1345.	1.5	29
29	Tongue Volume Influences Lowest Oxygen Saturation but Not Apnea-Hypopnea Index in Obstructive Sleep Apnea. PLoS ONE, 2015, 10, e0135796.	1.1	28
30	Incidentally Found Pharyngoesophageal Diverticulum on Ultrasonography. Yonsei Medical Journal, 2002, 43, 271.	0.9	27
31	Association between vestibular schwannomas and mobile phone use. Tumor Biology, 2014, 35, 581-587.	0.8	27
32	Efficacy and safety of vinorelbine plus cisplatin chemotherapy for patients with recurrent and/or metastatic salivary gland cancer of the head and neck. Head and Neck, 2018, 40, 55-62.	0.9	26
33	Extranodal nasal-type NK/T-cell lymphoma: Computed tomography findings of head and neck involvement. Acta Radiologica, 2010, 51, 164-169.	0.5	25
34	Establishment of a platform of non-small-cell lung cancer patient-derived xenografts with clinical and genomic annotation. Lung Cancer, 2018, 124, 168-178.	0.9	23
35	Spindle cell lipoma of the head and neck: CT and MR imaging findings. Neuroradiology, 2013, 55, 101-106.	1.1	22
36	Clinical Use of Diffusion Tensor Image-Merged Functional Neuronavigation for Brain Tumor Surgeries: Review of Preoperative, Intraoperative, and Postoperative Data for 123 Cases. Yonsei Medical Journal, 2014, 55, 1303.	0.9	22

#	Article	IF	CITATIONS
37	Machine Learning Based Radiomic <scp>HPV</scp> Phenotyping of Oropharyngeal <scp>SCC</scp> : A Feasibility Study Using <scp>MRI</scp> . Laryngoscope, 2021, 131, E851-E856.	1.1	22
38	Distinction between Intradural and Extradural Aneurysms Involving the Paraclinoid Internal Carotid Artery with T2-Weighted Three-Dimensional Fast Spin-Echo Magnetic Resonance Imaging. Journal of Korean Neurosurgical Society, 2010, 47, 437.	0.5	20
39	Evaluation of MRI Criteria for Cavernous Sinus Invasion in Pituitary Macroadenoma. Journal of Neuroimaging, 2014, 24, 498-503.	1.0	20
40	Effect of hypertension on the resting-state functional connectivity in patients with Alzheimer's disease (AD). Archives of Gerontology and Geriatrics, 2015, 60, 210-216.	1.4	20
41	An interpretable multiparametric radiomics model for the diagnosis of schizophrenia using magnetic resonance imaging of the corpus callosum. Translational Psychiatry, 2021, 11, 462.	2.4	20
42	Neuroradiologic findings in children with mitochondrial disorder: correlation with mitochondrial respiratory chain defects. European Radiology, 2008, 18, 1741-1748.	2.3	19
43	Diffusion-tensor magnetic resonance imaging in children with language impairment. NeuroReport, 2006, 17, 1279-1282.	0.6	18
44	Correlation of vestibular aqueduct size with air-bone gap in enlarged vestibular aqueduct syndrome. Laryngoscope, 2016, 126, 1633-1638.	1.1	18
45	Is there an additive value of 18 F-FDG PET-CT to CT/MRI for detecting nodal metastasis in oropharyngeal squamous cell carcinoma patients with palpably negative neck?. Acta Radiologica, 2016, 57, 1352-1359.	0.5	18
46	Mouse–human co-clinical trials demonstrate superior anti-tumour effects of buparlisib (BKM120) and cetuximab combination in squamous cell carcinoma of head and neck. British Journal of Cancer, 2020, 123, 1720-1729.	2.9	18
47	Initial Experiences with Proton MR Spectroscopy in Treatment Monitoring of Mitochondrial Encephalopathy. Yonsei Medical Journal, 2010, 51, 672.	0.9	17
48	Human Papillomavirus and Epidermal Growth Factor Receptor in Oral Cavity and Oropharyngeal Squamous Cell Carcinoma: Correlation With Dynamic Contrast-Enhanced MRI Parameters. American Journal of Roentgenology, 2016, 206, 408-413.	1.0	17
49	Visualization of maturation of the corpus callosum during childhood and adolescence using T2 relaxometry. International Journal of Developmental Neuroscience, 2007, 25, 409-414.	0.7	16
50	Measuring Fractional Anisotropy of the Corpus Callosum Using Diffusion Tensor Imaging: Mid-Sagittal versus Axial Imaging Planes. Korean Journal of Radiology, 2008, 9, 391.	1.5	16
51	Nasal polyps with metaplastic ossification: CT and MR imaging findings. Neuroradiology, 2010, 52, 1179-1184.	1.1	16
52	Prognostic Value of Cervical Nodal Necrosis Observed in Preoperative CT and MRI of Patients With Tongue Squamous Cell Carcinoma and Cervical Node Metastases: A Retrospective Study. American Journal of Roentgenology, 2019, 213, 437-443.	1.0	16
53	Internal Thoracic Artery Collateral to the External Iliac Artery in Chronic Aortoiliac Occlusive Disease. Korean Journal of Radiology, 2003, 4, 179.	1.5	15
54	Intracranial Dural Metastasis of Ewing's Sarcoma: a Case Report. Korean Journal of Radiology, 2008, 9, 76.	1.5	14

#	Article	IF	CITATIONS
55	Establishment and characterization of patient-derived xenografts as paraclinical models for head and neck cancer. BMC Cancer, 2020, 20, 316.	1.1	14
56	Pseudoaneurysm of the Inferior Thyroid Artery Presenting as a Thyroid Nodule. Thyroid, 2009, 19, 69-71.	2.4	13
57	Comparison between Ultrasonography and Computed Tomography for Detecting the Pyramidal Lobe of the Thyroid Gland: A Prospective Multicenter Study. Korean Journal of Radiology, 2015, 16, 402.	1.5	13
58	CT features of thyroid nodules with isolated macrocalcifications detected by ultrasonography. Ultrasonography, 2020, 39, 130-136.	1.0	12
59	Magnetic Resonance Imaging-Visible Perivascular Spaces in the Basal Ganglia Are Associated With the Diabetic Retinopathy Stage and Cognitive Decline in Patients With Type 2 Diabetes. Frontiers in Aging Neuroscience, 2021, 13, 666495.	1.7	11
60	¹⁸ <scp>F</scp> â€ <scp>FDG PET</scp> â€ <scp>CT</scp> as a supplement to <scp>CT</scp> / <scp>MRI</scp> for detection of nodal metastasis in hypopharyngeal <scp>SCC</scp> with palpably negative neck. Laryngoscope, 2015, 125, 1607-1612.	1.1	10
61	Detection of clinically occult primary tumours in patients with cervical metastases of unknown primary tumours: comparison of three-dimensional THRIVE MRI, two-dimensional spin-echo MRI, and contrast-enhanced CT. Clinical Radiology, 2018, 73, 410.e9-410.e15.	0.5	10
62	Use of Computed Tomography to Predict the Possibility of Exposure of the First Genu of the Facial Nerve Via the Transmastoid Approach. Otology and Neurotology, 2011, 32, 1180-1184.	0.7	8
63	Langerhans cell histiocytosis in endoscopic biopsy: marked pinching artifacts by endoscopy. Brain Tumor Pathology, 2011, 28, 285-289.	1.1	8
64	Clinical Usefulness of [18F]FDG PET-CT and CT/MRI for Detecting Nodal Metastasis in Patients with Hypopharyngeal Squamous Cell Carcinoma. Annals of Surgical Oncology, 2015, 22, 994-999.	0.7	8
65	Comparative evaluation of the white matter fiber integrity in patients with prelingual and postlingual deafness. NeuroReport, 2017, 28, 1103-1107.	0.6	8
66	Neural correlates of cricopharyngeal dysfunction after supratentorial stroke: A voxel-based lesion-symptom mapping with propensity score matched case–control. International Journal of Stroke, 2022, 17, 207-217.	2.9	8
67	Paratracheal Air Cysts: Sonographic Findings in Two Cases. Korean Journal of Radiology, 2003, 4, 136.	1.5	8
68	Retropharyngeal lymph node metastasis from olfactory neuroblastoma: a report of two cases. European Archives of Oto-Rhino-Laryngology, 2006, 263, 778-782.	0.8	7
69	Newly observed thalamic involvement and mutations of the HEXA gene in a Korean patient with juvenile GM2 gangliosidosis. Metabolic Brain Disease, 2008, 23, 235-242.	1.4	7
70	Tumor Markers in Fine-Needle Aspiration Washout for Cervical Lymphadenopathy in Patients With Known Malignancy: Preliminary Study. American Journal of Roentgenology, 2011, 197, W730-W736.	1.0	7
71	The Effect of Systemic Steroids and Orbital Radiation for Active Graves Orbitopathy on Postdecompression Extraocular Muscle Volume. American Journal of Ophthalmology, 2016, 171, 11-17.	1.7	7
72	Vibration-induced nystagmus in patients with vestibular schwannoma: Characteristics and clinical implications. Clinical Neurophysiology, 2017, 128, 1372-1379.	0.7	7

#	Article	IF	CITATIONS
73	Contrast-Enhanced CT with Knowledge-Based Iterative Model Reconstruction for the Evaluation of Parotid Gland Tumors: A Feasibility Study. Korean Journal of Radiology, 2018, 19, 957.	1.5	7
74	Hemorrhage in the endolymphatic sac: A cause of hearing fluctuation in enlarged vestibular aqueduct. International Journal of Pediatric Otorhinolaryngology, 2011, 75, 1538-1544.	0.4	6
75	Third Windows as a Cause of Failure in Hearing Gain after Exploratory Tympanotomy. Otolaryngology - Head and Neck Surgery, 2011, 145, 303-308.	1.1	6
76	The Feasibility of ¹⁸ F-fluorodeoxyglucose-positron Emission Tomography Uptake as a Prognostic Factor for Paranasal Sinus Malignancy. American Journal of Rhinology and Allergy, 2013, 27, 118-122.	1.0	6
77	Permeability Parameters Measured with Dynamic Contrast-Enhanced MRI: Correlation with the Extravasation of Evans Blue in a Rat Model of Transient Cerebral Ischemia. Korean Journal of Radiology, 2015, 16, 791.	1.5	6
78	Reduction of Oxygen-Induced CSF Hyperintensity on FLAIR MR Images in Sedated Children: Usefulness of Magnetization-Prepared FLAIR Imaging. American Journal of Neuroradiology, 2016, 37, 1549-1555.	1.2	6
79	MR lymphography for sentinel lymph node detection in patients with oral cavity cancer: Preliminary clinical study. Head and Neck, 2018, 40, 1483-1488.	0.9	6
80	Neural substrates for poststroke complex regional pain syndrome type I: a retrospective case–control study using voxel-based lesion symptom mapping analysis. Pain, 2020, 161, 1311-1320.	2.0	6
81	The feasibility of performing multiple burr hole surgery in pediatric moyamoya patients as a response to failed mEDAS. Child's Nervous System, 2021, 37, 2233-2238.	0.6	6
82	Squamous Cell Carcinoma and Lymphoma of the Oropharynx: Differentiation Using a Radiomics Approach. Yonsei Medical Journal, 2020, 61, 895.	0.9	6
83	Atopic Dermatitis With Group A β-Hemolytic Streptococcus Skin Infection Complicated by Posterior Reversible Encephalopathy Syndrome. Archives of Dermatology, 2009, 145, 846-7.	1.7	5
84	Accuracy of 3ÂT MR angioraphy in vertebral artery stenosis and coincidence with other cerebrovascular stenoses. Neuroradiology, 2010, 52, 893-898.	1.1	5
85	Subdural Fluid Collection After the Clipping of Unruptured Intracranial Aneurysms: Its Clinical Course and Significance. World Neurosurgery, 2018, 116, e266-e272.	0.7	5
86	An interpretable radiomics model for the diagnosis of panic disorder with or without agoraphobia using magnetic resonance imaging. Journal of Affective Disorders, 2022, 305, 47-54.	2.0	5
87	MR Findings of Fulminent Leukoencephalopathy in EBV-Associated Hemophagocytic Syndrome. Yonsei Medical Journal, 2006, 47, 873.	0.9	4
88	Antepartum Pituitary Necrosis Occurring In Pregnancy with Uncontrolled Gestational Diabetes Mellitus: A Case Report. Journal of Korean Medical Science, 2010, 25, 794.	1.1	4
89	Diffusion Tensor Imaging of Heterotopia: Changes of Fractional Anisotropy during Radial Migration of Neurons. Yonsei Medical Journal, 2010, 51, 590.	0.9	4
90	A biphasic tumor consisting of pilocytic astrocytoma with an anaplastic solitary fibrous tumor component in the pineal region: A case report and literature review. Neuropathology, 2013, 33, 288-291.	0.7	4

#	Article	IF	CITATIONS
91	Cinical Application of Iopamidol (Pamiray® 300) for Cerebral Angiography. Journal of the Korean Radiological Society, 2007, 57, 121.	0.0	4
92	Focal time-to-peak changes on perfusion MRI in children with Moyamoya disease: correlation with conventional angiography. Acta Radiologica, 2011, 52, 675-679.	0.5	3
93	Feasibility of a low-dose orbital CT protocol with a knowledge-based iterative model reconstruction algorithm for evaluating Graves' orbitopathy. Clinical Imaging, 2018, 51, 327-331.	0.8	3
94	Preoperative MRI Evaluation of Thyroid Cartilage Invasion in Patients with Laryngohypopharyngeal Cancer: Comparison of Contrast-Enhanced 2D Spin-Echo and 3D T1-Weighted Radial Gradient Recalled-Echo Techniques. American Journal of Neuroradiology, 2021, 42, 1690-1694.	1.2	3
95	Clinical factors and conventional MRI may independently predict progression-free survival and overall survival in adult pilocytic astrocytomas. Neuroradiology, 2022, 64, 1529-1537.	1.1	3
96	Transoral Robotic Surgery: Technical Review and Postoperative Imaging Findings. Neurographics, 2012, 2, 80-87.	0.0	2
97	Disproportional enrichment of FoxP3 ⁺ CD4 ⁺ regulatory T cells shapes a suppressive tumour microenvironment in head and neck squamous cell carcinoma. Clinical and Translational Medicine, 2022, 12, e753.	1.7	2
98	Radiology Quiz Case 1. JAMA Otolaryngology, 2010, 136, 1030.	1.5	1
99	Enlarged Superior Cervical Sympathetic Ganglion Mimicking a Metastatic Lymph Node in the Retropharyngeal Space: A Case Report. Journal of the Korean Society of Radiology, 2017, 76, 278.	0.1	0
100	Comparison of 3D Volumetric Subtraction Technique and 2D Dynamic Contrast Enhancement Technique in the Evaluation of Contrast Enhancement for Diagnosing Cushing's Disease. Investigative Magnetic Resonance Imaging, 2018, 22, 102.	0.2	0
101	CT Findings of Sporadic Cherubism in a 6-Year-Old Boy. Journal of the Korean Society of Radiology, 2014, 70, 13.	0.1	0
102	Salvage multiple burr hole surgery in patients with Moyamoya disease: efficacy evaluation using probabilistic independent component analysis of dynamic susceptibility contrast perfusion MRI. Neuroradiology, 2022, , 1.	1.1	0